Multiphoton states engineering by heralded interference via six-port Mach-Zehnder interferometer

Qiang Ke¹, Xue-feng Zhan¹, Min-xiang Li², and Xue-xiang Xu^{1,†}

¹College of Physics and Communication Electronics,

Jiangxi Normal University, Nanchang 330022, China;

²School of Education, Jiangxi Normal University,

Nanchang 330022, China

[†]xuxuexiang@jxnu.edu.cn

Based on heralded interference on a six-port Mach-Zehnder interferometer, we propose protocols to generate a series of multiphoton states in primary output port, by injecting a coherent state in primary input port and two Fock states in two ancillary input ports, and measuring two Fock states in two ancillary output ports. Only manipulating at the single-photon level (i.e, $|0\rangle$ or $|1\rangle$) in all ancillary ports, we generate sixteen types (six categories) of multiphoton nonclassical states, whose state vectors are unified as superposition of a new coherent state, a single-photon added coherent state, and a two-photon added coherent state. Indeed, a wide range of nonclassical phenomena can be created by modulating the interaction parameters (including coherent field strength and shift phase). We mainly analyze quadrature-squeezing effects for all our considered states. Of particular interest is maximum squeezing of up to 2.57dB, with success probability 6.7%, at least in our present cases.

I. INTRODUCTION

Many quantum phenomena are based on the principle of quantum interference, which lies at the heart of quantum theory[1–3]. Quantum interference has been widely applied in quantum technologies, such as quantum computation[4], quantum metrology[5], quantum teleporation[6] and quantum state engineering[7]. In previous years, there are many typical works on classical or quantum interference. The famous Yang's double-slit experiment demonstrated the interference effect of light[8]. The landmark HOM experiment demonstrated the two-photon interference based on a 50:50 beamsplitter[9]. The Knill-Laflamme-Milburn (KLM) scheme with photon interference revealed that efficient quantum computation is possible using only beam splitters, phase shifters, single-photon sources and photodetectors[10].

As we know, the beam splitter is a typical two-inputport splitter, which can be generalized to multi-port beam splitters, such as tritter and quarter[11]. Moreover, multi-port beam splitters are cornerstone devices for high-dimensional quantum information tasks[12]. Undeniably, these devices have their respective unitary operations, which can be modeled and implemented in the field of quantum optics[13]. Indeed, any unitary operation can be implemented by reconfigurable devices[14-16]. Following the construction of Mach-Zehnder interferometer (MZI), we can extend the generalized Mach-Zehnder structure, which can be realized by a chain of two subsequent multiport beam splitters. Thus, a multi-arm interferometer can be realized by cascading two multi-port beam splitters. Recently, Spagnolo et al. reported the experimental observation of three-photon interference in an integrated three-port directional couplers[17] and introduced three-dimensional (3D) multiphoton interferometry[18].

In the realm of quantum state engineering, many protocols are proposed to prepare quantum states via quantum interference. For example, Bartley developed a technique for generating multiphoton nonclassical states via interference between coherent and Fock states[19]. In one of our previous works, we proposed a scheme to generate nonclassical states from a coherent state heralded by KLM-type interference. The maximum squeezing of our generated states is about 1.97928dB[20]. In another work, based on a conditional interferometry proposed by Paris[21], we prepare any chosen superposition of the vacuum, one-photon, and two photon states[22]. Recently, Ripala et al. presented a theoretical study of the interferences between hybrid single-photon state, coherent state and vacuum state based on a six-port MZI (6p-MZI)[23].

In this work, we also consider using another 6p-MZI as the interference device and prepare quantum states by heralded method. The remaining paper is organized as follows. In Sec.2, we introduce the 6p-MZI including its device and transformation and then propose the generating protocol of multiphoton quantum states. In Sec.3 we give the unified forms of state vectors, density operators and success probabilities for all generated states considered in this work. Then in sec.4, we analyze the quadrature-squeezing effects for our considered quantum states. Conclusion is given in the last section.

II. GENERATING PROTOCOLS

We consider a 6p-MZI as shown in Fig.1, which is composed of tritter 1, phase shifter and tritter 2. Assuming these three devices can be described by operators \hat{T}_1 , \hat{P}_ϕ , and \hat{T}_2 , respectively. Their respective transfer matrices $U_{\hat{T}_2}$, $U_{\hat{P}_\phi}$, and $U_{\hat{T}_2}$ are given in Appendix A, where the tritters are symmetrical and lossless. Then, the 6p-MZI

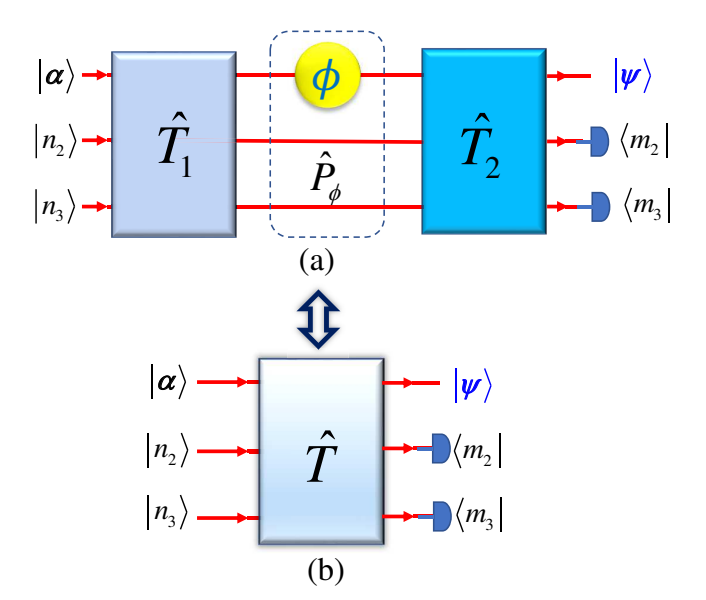


FIG. 1: (Colour online) (a) Schematic setup of 6p-MZI, which consist of tritter 1 (by operator \hat{T}_1), phase shifter (by operator \hat{P}_{ϕ}) and tritter 2 (by operator \hat{T}_2); (b) Equivalent of 6p-MZI (by operator $\hat{T}=\hat{T}_2\hat{P}_{\phi}\hat{T}_1$). By injecting $|\alpha\rangle$, $|n_2\rangle$, $|n_3\rangle$ in three input ports, and measuring $|m_2\rangle$ and $|m_3\rangle$ in two output ports, a new state $|\psi\rangle$ will be generated in another output port. In contrast with the input $|\alpha\rangle$, the output $|\psi\rangle$ will have a wide range of nonclassical properties.

can be described by operator $\hat{T} = \hat{T}_2 \hat{P}_{\phi} \hat{T}_1$ and satisfy

$$\hat{T} \begin{pmatrix} a_1^{\dagger} \\ a_2^{\dagger} \\ a_2^{\dagger} \end{pmatrix} \hat{T}^{\dagger} = U \begin{pmatrix} a_1^{\dagger} \\ a_2^{\dagger} \\ a_2^{\dagger} \end{pmatrix}, \tag{1}$$

with transfer matrix

$$U = U_{\hat{T}_2} U_{\hat{P}_{\phi}} U_{\hat{T}_1} = \begin{pmatrix} u_{11} & u_{12} & u_{13} \\ u_{21} & u_{22} & u_{23} \\ u_{31} & u_{32} & u_{33} \end{pmatrix},$$
(2)

where $u_{11}=u_{22}=u_{33}=\left(e^{-i\phi}+2\right)/3$ and $u_{12}=u_{21}=u_{13}=u_{31}=u_{23}=u_{32}=\left(e^{-i\phi}-1\right)/3$.

Based on the above 6p-MZI, we propose schemes to generate states according to the following procedure:

- (1) injecting coherent state $|\alpha\rangle$, Fock state $|n_2\rangle$ and Fock state $|n_3\rangle$ in the first, second and third input port, respectively; Here we assume $\alpha = |\alpha| e^{i\theta}$ with $\theta = 0$.
 - (2) interacting with interference in the 6p-MZI;
- (3) making perfect counting measurement with Fock state $|m_2\rangle$ and Fock state $|m_3\rangle$ in the second and third output port, respectively;
- (4) then generating a new quantum state $\left|\psi_{n_2n_3,\alpha,\phi}^{m_2m_3}
 ight.\rangle=\left|\psi
 ight.\rangle$ in the first output port.

Formally, the generating state can be expressed as

$$|\psi\rangle = \frac{1}{\sqrt{p_{n_2 m_3, \alpha, \phi}^{m_2 m_3}}} \langle m_3|_3 \langle m_2|_2 \hat{T} |\alpha\rangle_1 |n_2\rangle_2 |n_3\rangle_3 \quad (3)$$

with the success probability $p_{n_2n_3,\alpha,\phi}^{m_2m_3}$. By tuning the parameters of the interactions, namely, the Fock-state numbers n_2, n_3, m_2, m_3 , the shifted phase ϕ , and coherent-state amplitude α , a series of states can be generated. General analytical results for state vector, density operator, success probability, and expectation value for $|\psi\rangle$ can be obtained from results provided in Appendix B and Appendix C. It should be noted that operator a_1^{\dagger} (a_1) is directly written as a^{\dagger} (a).

III. CONSIDERED MULTIPHOTON STATES

Zero-photon operation and single-photon operation are known to dramatically alter the properties of certain quantum optical states [24, 25]. They have potential applications in the context of quantum communications and quantum information processing [26]. Enlighten by these ideas, we only consider by taking n_2 , n_3 , m_2 , $m_3 \in (0, 1)$ in our above protocol and study 16 types of generating states in this work. After our careful analysis, we find that their state vectors, density operators and success probabilities can be unified.

Unified state vectors: State vectors of all considered generating states can be unified as

$$|\psi_i\rangle = \frac{1}{\sqrt{N_i}} (c_{i0} + c_{i1}a^{\dagger} + c_{i2}a^{\dagger 2}) |u_{11}\alpha\rangle,$$
 (4)

with normalization factor

$$N_{i} = |c_{i0}|^{2} + |c_{i1}|^{2} + 2|c_{i2}|^{2} + (|c_{i1}|^{2} + 4|c_{i2}|^{2})|u_{11}|^{2}|\alpha|^{2} + |c_{i2}|^{2}|u_{11}|^{4}|\alpha|^{4} + 2\operatorname{Re}(c_{i0}c_{i2}^{*}u_{11}^{2}\alpha^{2}) + 2\operatorname{Re}[(c_{i0}c_{i1}^{*} + 2c_{i1}c_{i2}^{*})u_{11}\alpha] + 2\operatorname{Re}(c_{i1}c_{i2}^{*}|u_{11}|^{2}|\alpha|^{2}u_{11}\alpha).$$
 (5)

Here, c_{i0} , c_{i1} , and c_{i2} for each $|\psi_i\rangle$ are illustrated in Table I. These 16 states can be classified into the following 6 categories:

- (1) $|\psi_1\rangle$, $|\psi_2\rangle$, $|\psi_3\rangle$, and $|\psi_4\rangle$ are new CSs $|u_{11}\alpha\rangle$ (CS);
- (2) $|\psi_5\rangle$ and $|\psi_6\rangle$ are single-photon added CSs $a^\dagger\,|u_{11}\alpha\rangle$ (SPACS);
 - (3) $|\psi_7\rangle$ is a two-photon added CS $a^{\dagger 2}|u_{11}\alpha\rangle$ (TPACS);
- (4) $|\psi_8\rangle$, $|\psi_9\rangle$, $|\psi_{10}\rangle$, $|\psi_{11}\rangle$, $|\psi_{12}\rangle$, and $|\psi_{13}\rangle$ are superposition states of $|u_{11}\alpha\rangle$ and $a^{\dagger}|u_{11}\alpha\rangle$;
- (5) $|\psi_{14}\rangle$ and $|\psi_{15}\rangle$ are superposition states of $a^{\dagger}|u_{11}\alpha\rangle$ and $a^{\dagger 2}|u_{11}\alpha\rangle$;
- (6) $|\psi_{16}\rangle$ is a superposition state of $|u_{11}\alpha\rangle$, $a^{\dagger}|u_{11}\alpha\rangle$ and $a^{\dagger 2}|u_{11}\alpha\rangle$.

Unified density operators: Density operators ρ_j =

TABLE I: c_{i0} , c_{i1} , and c_{i2} for each $|\psi_i\rangle$. Note that $\tau_1 = u_{12}u_{23} + u_{13}u_{22}$, $\tau_2 = u_{12}u_{33} + u_{13}u_{32}$, $\tau_3 = u_{21}u_{32} + u_{22}u_{31}$, $\tau_4 = u_{21}u_{33} + u_{23}u_{31}$, $\tau_5 = u_{23}u_{32} + u_{22}u_{33}$, $\kappa = u_{12}u_{23}u_{31} + u_{13}u_{22}u_{31} + u_{13}u_{21}u_{32} + u_{12}u_{21}u_{33}$.

$\left \psi_{n_2n_3,\alpha,\phi}^{m_2m_3}\right\rangle$	$ \psi_i\rangle$	c_{i0}	c_{i1}	c_{i2}
$ \psi^{00}_{00,\alpha,\phi}\rangle$	$ \psi_1\rangle$	1	0	0
$ \psi_{00,\alpha,\phi}^{10}\rangle$	$ \psi_2\rangle$	$u_{12}\alpha$	0	0
$\left \psi_{00,\alpha,\phi}^{01}\right\rangle$	$ \psi_3\rangle$	$u_{13}\alpha$	0	0
$ \psi_{00,\alpha,\phi}^{11}\rangle$	$ \psi_4\rangle$	$u_{12}u_{13}\alpha^2$	0	0
$ \psi_{10,\alpha,\phi}^{00}\rangle$	$ \psi_5\rangle$	0	u_{21}	0
$\left \psi_{01,\alpha,\phi}^{00}\right\rangle$	$ \psi_6\rangle$	0	u_{31}	0
$ \psi_{11,\alpha,\phi}^{00}\rangle$	$ \psi_7\rangle$	0	0	$u_{21}u_{31}$
$\left \psi_{10,\alpha,\phi}^{10}\right\rangle$	$ \psi_8\rangle$	u_{22}	$u_{12}u_{21}\alpha$	0
$ \psi^{01}_{01,\alpha,\phi}\rangle$	$ \psi_9\rangle$	u_{33}	$u_{13}u_{31}\alpha$	0
$ \psi_{01,\alpha,\phi}^{10}\rangle$	$ \psi_{10}\rangle$	u_{32}	$u_{12}u_{31}\alpha$	0
$ \psi_{10,\alpha,\phi}^{01}\rangle$	$ \psi_{11}\rangle$	u_{23}	$u_{13}u_{21}\alpha$	0
$ \psi_{10,\alpha,\phi}^{11}\rangle$	$ \psi_{12}\rangle$	$ au_1 lpha$	$u_{12}u_{13}u_{21}\alpha^2$	0
$ \psi_{01,\alpha,\phi}^{11}\rangle$	$ \psi_{13}\rangle$	$ au_2 lpha$	$u_{12}u_{13}u_{31}\alpha^2$	0
$\left \psi_{11,\alpha,\phi}^{10}\right\rangle$	$ \psi_{14}\rangle$	0	$ au_3$	$u_{12}u_{21}u_{31}\alpha$
$ \psi_{11,\alpha,\phi}^{01}\rangle$	$ \psi_{15}\rangle$	0	$ au_4$	$u_{13}u_{21}u_{31}\alpha$
$ \psi_{11,\alpha,\phi}^{11}\rangle$	$ \psi_{16}\rangle$	$ au_5$	$\kappa \alpha$	$u_{12}u_{13}u_{21}u_{31}\alpha^2$

$|\psi_j\rangle\langle\psi_j|$ can be unified as

$$\rho_{i} = \frac{|c_{i0}|^{2}}{N_{i}} \rho^{(0,0)} + \frac{|c_{i1}|^{2}}{N_{i}} \rho^{(1,1)} + \frac{|c_{i2}|^{2}}{N_{i}} \rho^{(2,2)}$$

$$+ \frac{c_{i0}c_{i1}^{*}}{N_{i}} \rho^{(0,1)} + \frac{c_{i1}c_{i0}^{*}}{N_{i}} \rho^{(1,0)}$$

$$+ \frac{c_{i0}c_{i2}^{*}}{N_{i}} \rho^{(0,2)} + \frac{c_{i2}c_{i0}^{*}}{N_{i}} \rho^{(2,0)}$$

$$+ \frac{c_{i1}c_{i2}^{*}}{N_{i}} \rho^{(1,2)} + \frac{c_{i2}c_{i1}^{*}}{N_{i}} \rho^{(2,1)}.$$
(6)

for above 16 states after setting

$$\rho^{(h_l, h_r)} = a^{\dagger h_l} |u_{11}\alpha\rangle \langle u_{11}\alpha| a^{h_r}, \tag{7}$$

where h_l and h_r are non-negative integers. Thus, any property of ρ_i can be obtained from that of $\rho^{(h_l,h_r)}$ according to Eq.(6).

Unified success probabilities: Success probabilities of above generated states can be unified as

$$p_{n_2 n_3, \alpha, \phi}^{m_2 m_3} \longmapsto p_i = N_i e^{(|u_{11}|^2 - 1)|\alpha|^2}.$$
 (8)

In Fig.2 and Fig3, we plot all p_i s in the $(|\alpha|, \phi)$ space with $\phi \in [0, \pi]$, where different colors denote different categories. We find that even for the states in the same category, the success probability may be different. For example, in the first category $|u_{11}\alpha\rangle$ including four states $|\psi_1\rangle, |\psi_2\rangle, |\psi_3\rangle$, and $|\psi_4\rangle$, there are three different success probabilities, i.e., $p_1, p_2 = p_3$, and p_4 . In order to see

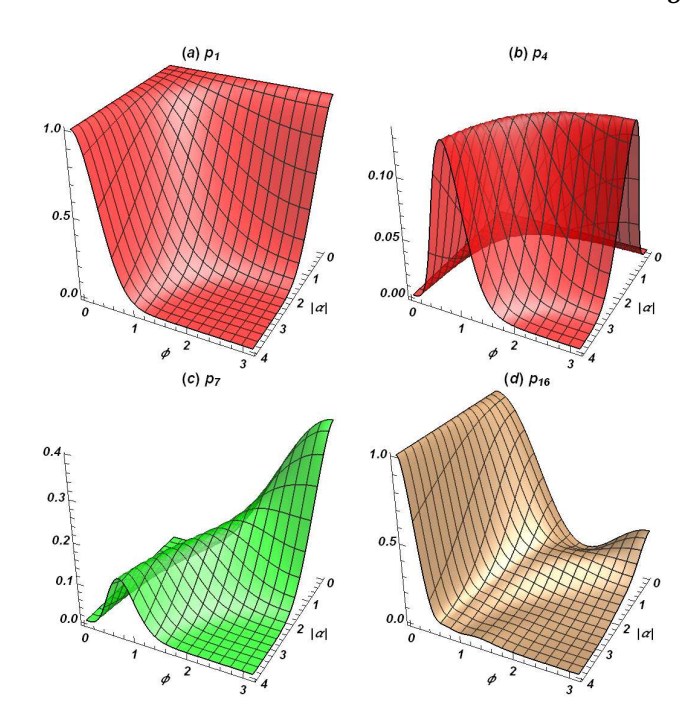


FIG. 2: Success probabilities in ($|\alpha|$, ϕ) space for states: (a) $|\psi_1\rangle$; (b) $|\psi_4\rangle$; (c) $|\psi_7\rangle$; (d) $|\psi_{16}\rangle$.

clearly the curves in above three-dimensional plots, we take $|\alpha|=2$ as example and plot each p_i as a function of ϕ in Fig.4. In the interval of $[0,2\pi]$, the probabilities are symmetrical on $\phi=\pi$.

IV. QUADRATURE-SQUEEZING EFFECTS

Quadrature-squeezing effects can be judged from that the \hat{x} -quadrature variance $\langle (\Delta \hat{x})^2 \rangle$ below the standard limit 0.5, where $\hat{x} = (a + a^\dagger)/\sqrt{2}$. That is, a state is quadrature-squeezing if $\langle (\Delta \hat{x})^2 \rangle < 0.5$ [27]. Obviously, $\langle (\Delta \hat{x})^2 \rangle = 0.5$ is always right for $|\psi_1\rangle$, $|\psi_2\rangle$, $|\psi_3\rangle$, and $|\psi_4\rangle$. But for states from $|\psi_5\rangle$ to $|\psi_{16}\rangle$, are they quadrature-squeezing? Fig.5 and Fig.6(a) presents their feasibility squeezing regions in the $(|\alpha|, \phi)$ space. Further, as examples, we plot $\langle (\Delta \hat{x})^2 \rangle$ s of $|\psi_{16}\rangle$ with $|\alpha| = 2, 4, 6$ as functions of ϕ in Fig.6(b).

The quadrature variance $\left<(\Delta\hat{x})^2\right>$ of a state, relative to the vacuum noise level of 0.5, can show squeezing degree by a logarithmic scale (units of dB) through $-10\log_{10}\left(\left<(\Delta\hat{x})^2\right>/0.5\right)$. In order to see the maximum squeezing degrees for states from $|\psi_5\rangle$ to $|\psi_{16}\rangle$, we use the computing software (MATHEMATICA) to find the minimize $\left<(\Delta\hat{x})^2\right>$ values under the constraints $0 \le |\alpha| \le 10$ and $0 \le \phi \le 2\pi$. The numerical or analytical results show that:

- (1) For states $|\psi_1\rangle$, $|\psi_2\rangle$, $|\psi_3\rangle$, and $|\psi_4\rangle$, the squeezing degrees are 0dB, showing without squeezing, because they are all coherent states;
- (2) For states including $|\psi_5\rangle$, $|\psi_6\rangle$, $|\psi_8\rangle$, $|\psi_9\rangle$, $|\psi_{10}\rangle$, $|\psi_{11}\rangle$, $|\psi_{12}\rangle$, and $|\psi_{13}\rangle$, their minimum variances (\sim

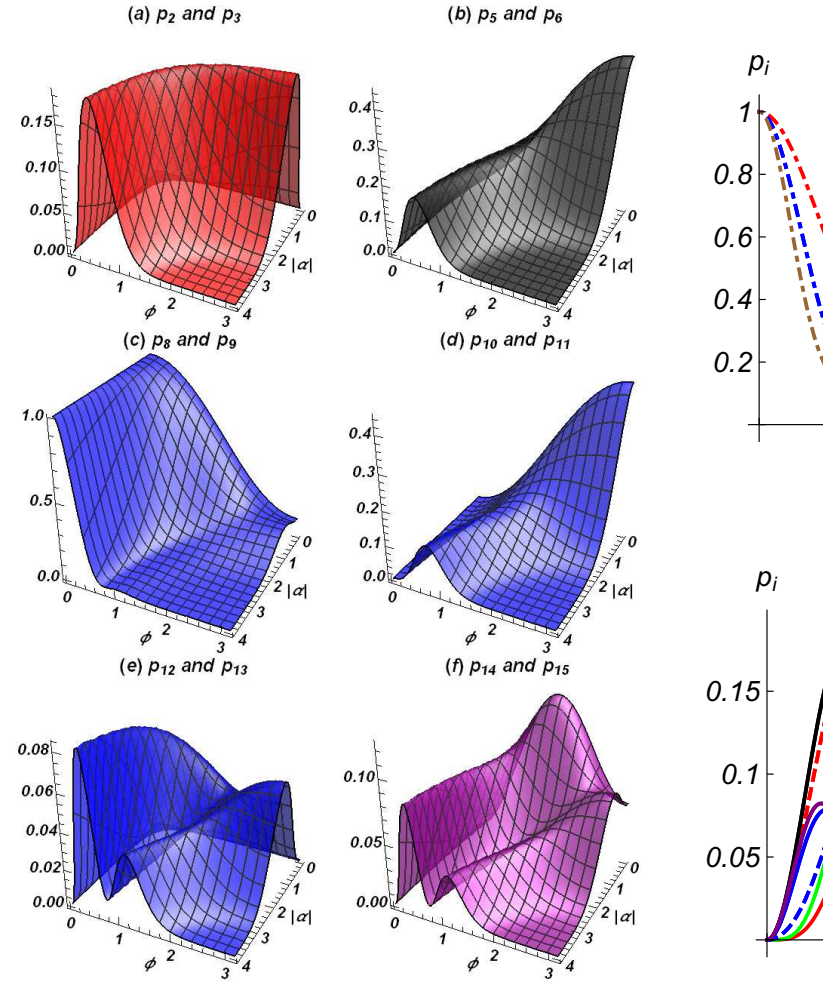


FIG. 3: Success probabilities in ($|\alpha|$, ϕ) space for states: (a) $|\psi_{2,3}\rangle$; (b) $|\psi_{5,6}\rangle$; (c) $|\psi_{8,9}\rangle$; (d) $|\psi_{10,11}\rangle$; (e) $|\psi_{12,13}\rangle$; (f) $|\psi_{14,15}\rangle$.

0.375) correspond to 1.25dB squeezing;

- (3) For states including $|\psi_7\rangle$, $|\psi_{14}\rangle$, and $|\psi_{15}\rangle$, their minimum variances (~ 0.322) correspond to about 1.91dB squeezing;
- (4) For state $|\psi_{16}\rangle$, its minimum variance (~ 0.277) corresponds to 2.57dB squeezing.

Interestingly, squeezing degrees with 1.91 dB and 2.57 dB are meaningful results in our proposals. Compared with the 1.25 dB squeezing degree in the Bartley's work[19], these maximum squeezing degrees have been greatly improved. Moreover, the success probability to obtain 2.57 dB squeezing can reach 6.7%.

Since the \hat{p} -quadratures are never squeezed for each $|\psi_i\rangle$, we don't discuss \hat{p} -quadrature variance $\langle (\Delta \hat{p})^2 \rangle$, with $\hat{p} = (a - a^{\dagger})/(i\sqrt{2})$.

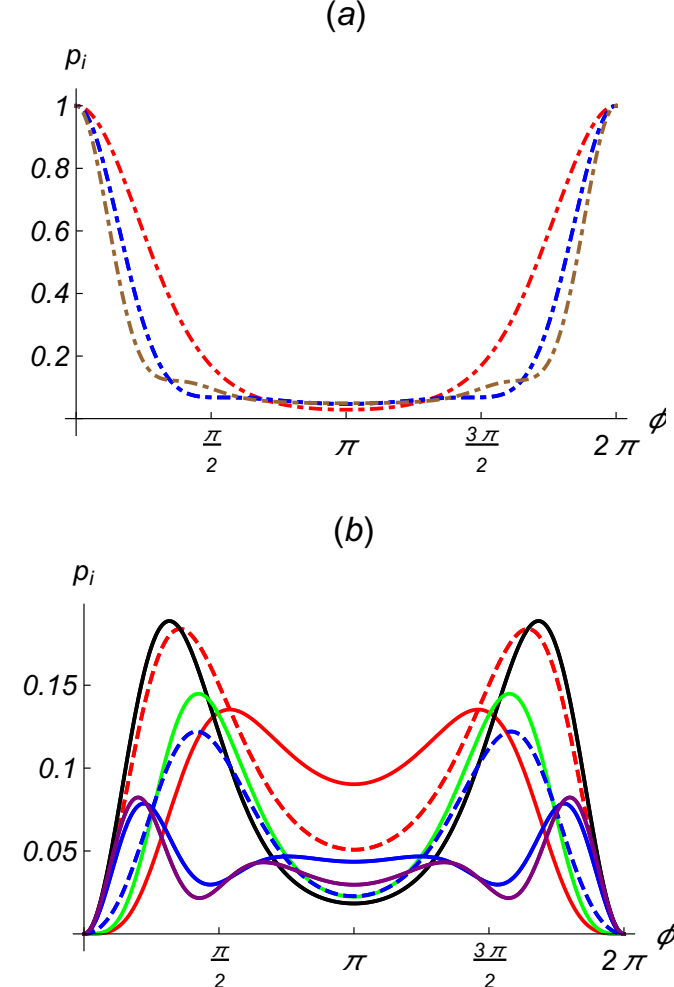


FIG. 4: (a) p_i as a function of ϕ , with $|\alpha|=2$ for $|\psi_1\rangle$ (red dotdashed), $|\psi_{8,9}\rangle$ (blue dotdashed), and $|\psi_{16}\rangle$ (brown dotdashed); (b) p_i as a function of ϕ , with $|\alpha|=2$ for $|\psi_{2,3}\rangle$ (red dashed), $|\psi_4\rangle$ (red), $|\psi_{5,6}\rangle$ (black), $|\psi_7\rangle$ (green), $|\psi_{10,11}\rangle$ (blue dashed), $|\psi_{12,13}\rangle$ (blue), and $|\psi_{14,15}\rangle$ (purple).

V. CONCLUSION

16 types of multiphoton states have been produced by available schemes based on a given 6p-MZI. Of course, these 16 states can be classified into 6 categories, according to their components of CS, SPACS and TPACS. Moreover, we analytically unified their state vectors, density operators, success probabilities. We numerically analyzed \hat{x} -squeezing effects and found that a maximum squeezing degree with 2.57dB can be obtained. In fact, many other interesting phenomena can be exhibited by taking different parameters. In view of the complexity and difficulty of calculation, we don't consider cases with bigger n_2 , n_3 , m_2 , m_3 in this work. However, we don't considered arbitrary devices with asymmetrical tritters.

Rather than application in quantum state engineering, these multiport splitters can also be applied in quantum simulations[28], linear optical computing[29] and non-

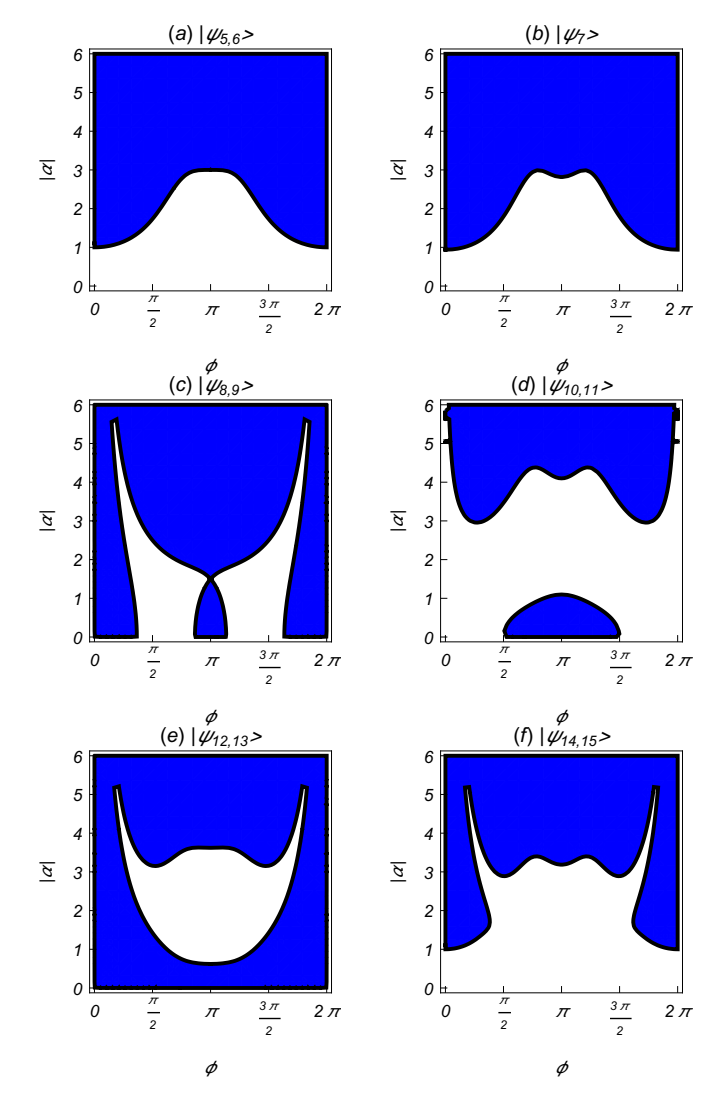


FIG. 5: Feasibility \hat{x} -squeezing effects in ($|\alpha|$, ϕ) space for states from $|\psi_5\rangle$ to $|\psi_{15}\rangle$, showing by blue regions.

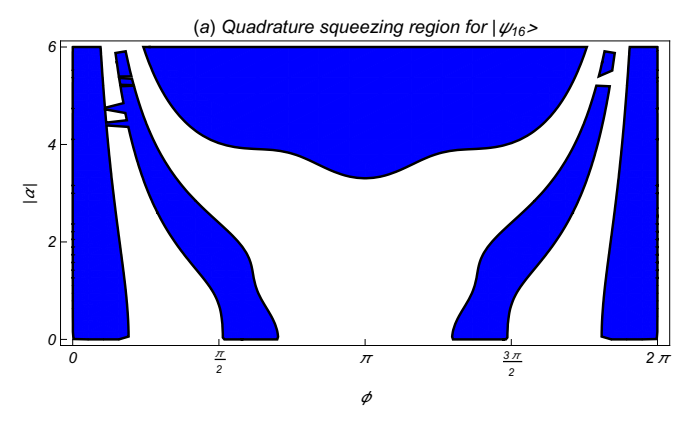
locality tests[30]. They will be important tools in quantum fields. We believe that the subject of multiport splitters will become a very active area of research.

Appendix A: Devices and transformations

We introduce devices and transformations used in our present scheme.

(1) Tritter 1: Transformation of Tritter 1 is described by

$$\hat{T}_1 \begin{pmatrix} a_1^{\dagger} \\ a_2^{\dagger} \\ a_3^{\dagger} \end{pmatrix} \hat{T}_1^{\dagger} = U_{\hat{T}_1} \begin{pmatrix} a_1^{\dagger} \\ a_2^{\dagger} \\ a_3^{\dagger} \end{pmatrix}, \tag{A.1}$$



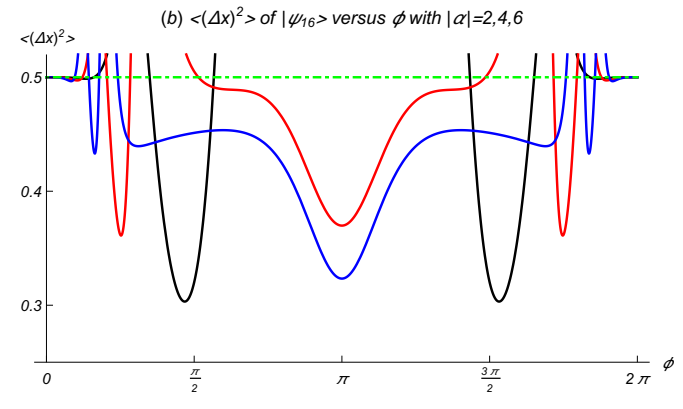


FIG. 6: (a) Feasibility \hat{x} -squeezing effects in $(|\alpha|, \phi)$ space for state $|\psi_{16}\rangle$, see blue region; (b) $\langle (\Delta \hat{x})^2 \rangle$ as a function of ϕ for state $|\psi_{16}\rangle$ with $|\alpha|=2,4,6$.

with transfer matrix

$$U_{\hat{T}_1} = \frac{1}{\sqrt{3}} \begin{pmatrix} 1 & 1 & 1\\ 1 & e^{i\frac{2\pi}{3}} & e^{i\frac{4\pi}{3}}\\ 1 & e^{i\frac{4\pi}{3}} & e^{i\frac{2\pi}{3}} \end{pmatrix}$$
(A.2)

(2) Phase shifter: Transformation of phase shifter is described by

$$\hat{P}_{\phi} \begin{pmatrix} a_1^{\dagger} \\ a_2^{\dagger} \\ a_3^{\dagger} \end{pmatrix} \hat{P}_{\phi}^{\dagger} = U_{\hat{P}_{\phi}} \begin{pmatrix} a_1^{\dagger} \\ a_2^{\dagger} \\ a_3^{\dagger} \end{pmatrix}, \tag{A.3}$$

with transfer matrix

$$U_{\hat{P}_{\phi}} = \begin{pmatrix} e^{-i\phi} & 0 & 0\\ 0 & 1 & 0\\ 0 & 0 & 1 \end{pmatrix} \tag{A.4}$$

(3) Tritter 2: Transformation of Tritter 2 is described by

$$\hat{T}_2 \begin{pmatrix} a_1^{\dagger} \\ a_2^{\dagger} \\ a_3^{\dagger} \end{pmatrix} \hat{T}_2^{\dagger} = U_{\hat{T}_2} \begin{pmatrix} a_1^{\dagger} \\ a_2^{\dagger} \\ a_3^{\dagger} \end{pmatrix}, \tag{A.5}$$

with transfer matrix

$$U_{\hat{T}_2} = \frac{1}{\sqrt{3}} \begin{pmatrix} 1 & 1 & 1\\ 1 & e^{i\frac{4\pi}{3}} & e^{i\frac{2\pi}{3}}\\ 1 & e^{i\frac{2\pi}{3}} & e^{i\frac{4\pi}{3}} \end{pmatrix}$$
(A.6)

Appendix B: About generated states

In this appendix, we give the general expression of state vector, density operator and success probability for all generated states.

(1) State vector: Noting $|\alpha\rangle=e^{-|\alpha|^2/2}e^{\alpha a_1^\dagger}|0\rangle_1$, $|n_j\rangle=(n_j!)^{-1/2}\,\partial_{s_j}^{n_j}\,e^{s_ja_j^\dagger}|0\rangle_j\,|_{s_j=0}$, and $\langle m_j|=(m_j!)^{-1/2}\,\partial_{t_j}^{m_j}\,\langle 0|_j\,e^{t_ja_j}|_{t_j=0}$, and using the transformation in Eq.(1) and $\hat{T}\,|0\rangle_1\,|0\rangle_2\,|0\rangle_3=|0\rangle_1\,|0\rangle_2\,|0\rangle_3$, we obtain

$$|\psi\rangle = \frac{e^{-\frac{|\alpha|^2}{2}}}{\sqrt{m_3! m_2! n_2! n_3! p_{n_2 n_3, \alpha, \phi}^{m_2 m_3}}} \partial_{s_2}^{n_2} \partial_{s_3}^{n_3} \partial_{t_2}^{m_2} \partial_{t_3}^{m_3}$$

$$e^{t_2(\alpha u_{12} + s_2 u_{22} + s_3 u_{32}) + t_3(\alpha u_{13} + s_2 u_{23} + s_3 u_{33})}$$

$$e^{(\alpha u_{11} + s_2 u_{21} + s_3 u_{31}) a_1^{\dagger}} |0\rangle_1|_{(s_2, t_2, s_3, t_3) = 0}$$
(B.1)

whose conjugate state is

$$\langle \psi | = \frac{e^{-\frac{|\alpha|^2}{2}}}{\sqrt{m_3! m_2! n_2! n_3! p_{n_2 n_3, \alpha, \phi}^{m_2 m_3}}} \partial_{f_2}^{n_2} \partial_{f_3}^{n_3} \partial_{g_2}^{m_2} \partial_{g_3}^{m_3}$$

$$e^{g_2(\alpha^* u_{12}^* + f_2 u_{22}^* + f_3 u_{32}^*) + g_3(\alpha^* u_{13}^* + f_2 u_{23}^* + f_3 u_{33}^*)}$$

$$\langle 0 |_1 e^{(\alpha^* u_{11}^* + f_2 u_{21}^* + f_3 u_{31}^*) a_1} |_{(f_2, g_2, f_3, g_3) = 0}. \tag{B.2}$$

(2) Density operator: The general density operator $\rho = |\psi\rangle\langle\psi|$ can be written as

$$\begin{split} \rho &= \frac{e^{-|\alpha|^2}}{m_3! m_2! n_2! n_3! p_{n_2 n_3, \alpha, \phi}^{m_2 m_3}} \\ \partial_{s_2}^{n_2} \partial_{s_3}^{n_3} \partial_{t_2}^{m_2} \partial_{t_3}^{m_3} \partial_{f_2}^{n_2} \partial_{f_3}^{n_3} \partial_{g_2}^{m_2} \partial_{g_3}^{m_3} \\ e^{t_2(\alpha u_{12} + s_2 u_{22} + s_3 u_{32}) + t_3(\alpha u_{13} + s_2 u_{23} + s_3 u_{33})} \\ e^{g_2(\alpha^* u_{12}^* + f_2 u_{22}^* + f_3 u_{32}^*) + g_3(\alpha^* u_{13}^* + f_2 u_{23}^* + f_3 u_{33}^*)} \\ e^{(\alpha u_{11} + s_2 u_{21} + s_3 u_{31}) a_1^{\dagger}} |0\rangle_1 \left\langle 0|_1 e^{(\alpha^* u_{11}^* + f_2 u_{21}^* + f_3 u_{31}^*) a_1} \right. \\ |_{(s_2, t_2, s_3, t_3, f_2, g_2, f_3, g_3) = 0}. \end{split} \tag{B.3}$$

(3) Success probability: Due to $Tr \rho = 1$, we obtain the success probability

$$\begin{split} p_{n_2n_3,\alpha,\phi}^{m_2m_3} &= \frac{e^{-|\alpha|^2}}{m_3! m_2! n_2! n_3!} \\ & \partial_{s_2}^{n_2} \partial_{s_3}^{n_3} \partial_{t_2}^{m_2} \partial_{t_3}^{m_3} \partial_{f_2}^{n_2} \partial_{f_3}^{n_3} \partial_{g_2}^{m_2} \partial_{g_3}^{m_3} \\ & e^{t_2(\alpha u_{12} + s_2 u_{22} + s_3 u_{32}) + t_3(\alpha u_{13} + s_2 u_{23} + s_3 u_{33})} \\ & e^{g_2(\alpha^* u_{12}^* + f_2 u_{22}^* + f_3 u_{32}^*) + g_3(\alpha^* u_{13}^* + f_2 u_{23}^* + f_3 u_{33}^*)} \\ & e^{(\alpha^* u_{11}^* + f_2 u_{21}^* + f_3 u_{31}^*)(\alpha u_{11} + s_2 u_{21} + s_3 u_{31})} \\ & |_{(s_2, t_2, s_3, t_3, f_2, g_2, f_3, g_3) = 0}. \\ & \mathbf{Appendix C: Calculation of} \langle a^{\dagger k} a^l \rangle_{\rho} \end{split}$$

In this appendix, we provide two ways to calculate $\langle a^{\dagger k}a^l\rangle_{\rho}.$

(1) Way 1: Using ρ in Eq.(B.3), we have

$$\langle a^{\dagger k} a^{l} \rangle_{\rho} = \frac{e^{-|\alpha|^{2}}}{m_{3}! m_{2}! n_{2}! n_{3}! p_{n_{2}n_{3},\alpha,\phi}^{m_{2}}}$$

$$\partial_{s_{2}}^{n_{2}} \partial_{s_{3}}^{n_{3}} \partial_{t_{2}}^{m_{2}} \partial_{t_{3}}^{m_{3}} \partial_{f_{2}}^{n_{2}} \partial_{f_{3}}^{n_{3}} \partial_{g_{2}}^{m_{2}} \partial_{g_{3}}^{m_{3}} \partial_{\mu}^{k} \partial_{\nu}^{l}$$

$$e^{t_{2}(\alpha u_{12} + s_{2} u_{22} + s_{3} u_{32}) + t_{3}(\alpha u_{13} + s_{2} u_{23} + s_{3} u_{33})}$$

$$e^{g_{2}(\alpha^{*} u_{12}^{*} + f_{2} u_{22}^{*} + f_{3} u_{32}^{*}) + g_{3}(\alpha^{*} u_{13}^{*} + f_{2} u_{23}^{*} + f_{3} u_{33}^{*})}$$

$$e^{(\nu + f_{2} u_{21}^{*}) \alpha u_{11} + (\mu + s_{2} u_{21}) \alpha^{*} u_{11}^{*} + (\nu + f_{3} u_{31}^{*}) s_{2} u_{21}}$$

$$e^{(\mu + s_{3} u_{31}) f_{2} u_{21}^{*} + (\nu + \alpha^{*} u_{11}^{*}) s_{3} u_{31} + (\mu + \alpha u_{11}) f_{3} u_{31}^{*}}$$

$$e^{+f_{2} s_{2} |u_{21}|^{2} + f_{3} s_{3} |u_{31}|^{2} + |\alpha|^{2} |u_{11}|^{2}}$$

$$|(f_{2}, g_{2}, f_{3}, g_{3}, s_{2}, t_{2}, s_{3}, t_{3}, \mu, \nu) = 0.$$
(C.1)

Thus, we can obtain arbitrary $\langle a^{\dagger k} a^l \rangle$ for each $|\psi_i\rangle$ by taking proper n_2, n_3, m_2, m_3 .

(2) Way 2: Using $\rho^{(h_l,h_r)}$, we first have

$$\begin{split} \left\langle a^{\dagger k} a^l \right\rangle_{\rho^{(h_l,h_r)}} &= \partial_s^{h_l} \partial_t^{h_r} \partial_\mu^k \partial_\nu^l e^{s\nu + t\mu + st} \\ &e^{(\nu + t)u_{11}\alpha + (s + \mu)u_{11}^*\alpha^*}|_{(\mu,\nu,s,t) = 0}. \end{split} \tag{C.2}$$

and then obtain $\langle a^{\dagger k} a^l \rangle_{\rho}$ according to Eq.(6).

Acknowledgments

This study was supported by the National Natural Science Foundation of China (No. 11665013).

- [1] M. Tillmann, S. -H. Tan, S. E. Stoeckl, B. C. Sanders, H. de Guise, R. Heilmann, S. Nolte, A. Szameit, and P. Walther, Generalized Multiphoton Quantum Interference, Phys. Rev. X 5, 041015 (2015)
- [2] A. J. Menssen, A. E. Jones, B. J. Metcalf, M. C. Tichy, S. Barz, W. Steven Kolthammer, and I. A. Walmsley, Distinguishability and Many-Particle Interference, Phys. Rev.
- Lett. 118, 153603 (2017).
- [3] A. J. Menssen, Multi-photon interference phenomena, A PhD these of University of Oxford, 2019; arXiv:2209.02893 (2019).
- [4] H. S. Zhong, H. Wand, Y. H. Deng, M. C. Chen, L. C. Peng, Y. H. Luo, J. Qin, Dian Wu, X. Ding, Y. Hu, P. Hu, X. Y. Yang, W. J. Zhang, Hao Li, Y. X. Li, X. Jiang, L. Gan, G. W.

- Yang, L. X. You, Z. Wand, L. Li, N. L. Liu, C. Y. Lu and J. W. Pan, quantum computational advantageous using photon, Science 370, 1460-1463 (2020).
- [5] V. Giovannetti, S. Lloyd, and L. Maccone, Quantum Metrology, Phys. Rev. Lett. 96, 010401 (2006).
- [6] Y. H. Luo, H. S. Zhong, M. Erhard, X. L. Wang, L. C. Peng, M. Krenn, X. Jiang, L. Li, N. L. Liu, C. Y. Lu, A. Zeilinger, and J. W. Pan, Quantum Teleportation in High Dimensions, Phys. Rev. Lett. 123, 070505 (2019).
- [7] L. Cui, Jie Su, J. M. Li, Y. H. Liu, X. Y. Li, and Z. Y. Ou, Quantum state engineering by nonlinear quantum interference, Phys. Rev. A 102, 033718 (2020).
- [8] A. Einstein, Uber einen die Erzeugung and Verwandlung des Lichtes betreffenden heuristischen Gesichtspunkt, Annalen der physik, 322, 132-148 (1905).
- [9] C. K. Hong, Z. Y. Ou, and L. Mandel, Measurement of subpicosecond time intervals between two photons by interference, Phys. Rev. Lett. 59, 2044-2046 (1987).
- [10] E. Knill, R. Laflamme, and G. J. Milburn, A schem for efficient quantum computation with linear optics, Nature, 409, 46-52 (2001).
- [11] M. Yu. Saygin, I. V. Kondratyev, I. V. Dyakonov, S. A. Mironov, S. S. Straupe, and S. P. Kulik, Robust architecture for programmable universal unitaries, Phys. Rev. Lett. 124, 010501 (2020).
- [12] M. Zukowski, A. Zeilinger, and M. A. Horne, Realizable higher-dimensional two-particle entanglement via multiport beam splitters, Phys. Rev. A 55, 2564-2579 (1997).
- [13] N. Tischer, C. Rockstuhl, and K. Slowik, Quantum optical realization of arbitrary linear transformations allowing for loss and gain, Phys. Rev. X 8, 021017 (2018).
- [14] M. Reck, A. Zeilinger, H. J. Bernstein, and P. Bertani, Experimental realization of any discrete unitary operator, Phys. Rev. Lett. 73, 58-61 (1994).
- [15] L. Pereira, A. Rojas, G. Canas, G. Lima, A. Delgado, A. Cabello, Minimum optical depth multi-port interferometers for approximating any unitary transformation and any pure state, arXiv: 2002.01371 (2020).
- [16] M. Z. Zhang, S. Chowdhury, L. Jiang, Universal interference-based construction of Gaussian operations in hybrid quantum systems, arXiv: 2112.08208 (2021).
- [17] N. Spagnolo, L. Aparo, C. Vitelli, A. Crespi, R. Ramponi, R. Osellame, P. Mataloni, and F. Sciarrino, Quantum in-

- terferometry with three-dimensional geometery, Sci. Rep. 2, 862 (2012).
- [18] N. Spagnolo, C. Vitelli, L. Aparo, P. Mataloni, F. Sciarrino, A. Crespi, R. Ramponi, and R. Osellame, Three-photon bosonic coalescence in an integrated tritter, Nat. Commun. 4, 1606 (2013).
- [19] T. J. Bartley, G. Donati, J. B. Spring, X. -M, Jin, M. Barbieri, A. Datta, B. J. Smith, and I. A. Walmsley, Multiphoton state engineering by heralded interference between single photons and coherent states, Phys. Rev. A 86, 043820 (2012).
- [20] X. X. Xu, H. C. Yuan, and S. J. Ma, Measurement-induced nonclassical states from a coherent state heralded by Knill-Laflamme-Milburn-type interference, J. Opt. Soc. Am. B 33, 061322 (2022).
- [21] M. G. A. Paris, Optical qubit by conditional interferometry, Phys. Rev. A 62, 033813 (2000).
- [22] X. X. Xu and H. C. Yuan, Coherent state truncation by conditional interferometry, Mod. Phys. Let. A 35, 2050158 (2020).
- [23] D. P. Ripala, Suryadi, and A. Y. Rohedi, Hybrid singlephoton, coherent, and vacuum states interference in the six-ports Mach-Zehnder interferometer, Journal of Physics: Conference Series, 1951, 012049 (2021).
- [24] C. M. Nunn, J. D. Franson, and T. B. Pittman, Heralding on the detection of zero photons, Phys. Rev. A 104, 033717 (2021).
- [25] C. M. Nunn, J. D. Franson, and T. B. Pittman, Modifying quantum optical states by zero-photon subtraction, Phys. Rev. A 105, 033702 (2022).
- [26] R. A. Brewster, I. C. Nodurft, T. B. Pittman, and J. D. Franson, Noiseless attenuation using an optical parametric amplifier, Phys. Rev. A 96, 042307 (2017).
- [27] C. C. Gerry and P. L. Knight, Introductory Quantum Optics, Cambridge University, Cambridge, England (2005).
- [28] S. Lloyd, Universal quantum simulators, Science 273, 1073-1078 (1996).
- [29] S. Aaronson and A Arkhipov, The computational complexity of linear optics, arXiv: 1011.3245 (2010).
- [30] J. Gruca, W. Laskowski, M. Zukowski, Nonclassicality of pure two-quidrit entangled states, Phys. Rev. A 85, 022118 (2012).